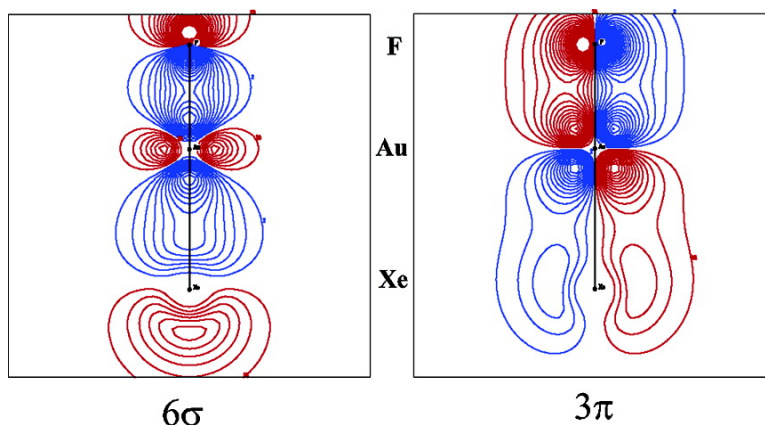


XeAuF

Stephen A. Cooke, and Michael C. L. Gerry

J. Am. Chem. Soc., **2004**, 126 (51), 17000-17008 • DOI: 10.1021/ja044955j • Publication Date (Web): 04 December 2004

Downloaded from <http://pubs.acs.org> on April 5, 2009



More About This Article

Additional resources and features associated with this article are available within the HTML version:

- Supporting Information
- Links to the 3 articles that cite this article, as of the time of this article download
- Access to high resolution figures
- Links to articles and content related to this article
- Copyright permission to reproduce figures and/or text from this article

[View the Full Text HTML](#)

XeAuF

Stephen A. Cooke* and Michael C. L. Gerry*

*Contribution from the Department of Chemistry, The University of British Columbia,
2036 Main Mall, Vancouver, B.C., Canada V6T 1Z1*

Received August 20, 2004; E-mail: mgerry@chem.ubc.ca; saccoke@chem.ubc.ca

Abstract: XeAuF has been detected and characterized using microwave rotational spectroscopy. It was prepared by laser ablation of Au in the presence of Xe and SF₆, and stabilized in a supersonic jet of Ar. The spectrum was measured with a cavity pulsed jet Fourier transform microwave spectrometer, in the frequency range 6–26 GHz. Rotational constants, centrifugal distortion constants, and ¹³¹Xe and ¹⁹⁷Au nuclear quadrupole coupling constants have been evaluated. The molecule is linear, with a short XeAu bond (2.54 Å), and is rigid. The ¹³¹Xe nuclear quadrupole coupling constant (NQCC) is large (–135 MHz). The ¹⁹⁷Au NQCC differs radically from that of uncomplexed AuF. The results are supported by those of ab initio calculations which have given an XeAu dissociation energy ~100 kJ mol⁻¹, plus Mulliken and natural bond orbital populations, MOLDEN plots of valence orbitals, and an energy density distribution. All evidence is consistent with XeAu covalent bonding in XeAuF.

1. Introduction

Only a few years ago, the existence of a triatomic molecule in which both Xe and F are directly and strongly bonded to Au would have been considered improbable. Even today its existence may take some chemists by surprise. There are two main issues. First, AuF was for many years considered a “nonexistent compound”.^{1–3} Only recently, and in the gas phase, have its existence been verified and its properties characterized.^{4,5} Second, there is the XeAu interaction in the context of noble gas–metal chemistry, which is an active and expanding field.^{6–9} Many noble gas–metal bonds are unexpectedly strong, prompting the question of whether they should be considered chemical bonds. An answer is obscure because of the lack of a clear definition of such bonds, which can prompt heated controversy.^{10–12} Experimental data on XeAuF would be of great value in considerations of molecular stability, relativistic effects, noble gas chemistry, and chemical bonding. Ideally such data would include information not only on its geometry, but also on the electron distributions at both Xe and Au in the complex.

Over the past five years we have reported the preparation and characterization of a series of noble gas–noble metal halide complexes. Their general formula is NgMX, with Ng = Ar, Kr, Xe; M = Cu, Ag, Au; X = F, Cl, Br.^{13–21} They were

generated by laser ablation of the metal in the presence of a suitable precursor, and stabilized in a supersonic jet of Ar. Detection and characterization were carried out by rotational spectroscopy, using a cavity pulsed jet Fourier transform microwave (FTMW) spectrometer.

These complexes, which are linear, have several unanticipated properties. The NgM bonds are short and rigid. Nuclear quadrupole coupling constants of ⁸³Kr, ¹³¹Xe, Cu, and Au indicate major reorganization of electron distributions on complex formation. Ab initio dissociation energies are large,²² and are found to be proportional to experimental NgM stretching force constants. The ab initio calculations also reveal occupied valence molecular orbitals (MOs) with electron density shared between Ng and M atoms, and significant donation of electron density from Ng to M. At first glance it would appear that the NgM bonds are at the border between van der Waals and chemical bonds. Previous results suggest that the nature of the NgM bonding is seemingly dependent mostly on the metal: the complexes containing Ag appear to show mostly van der Waals bonding, those containing Cu are intermediate, and those containing Au show distinct chemical bonding characteristics. The presence of ArAu and KrAu chemical bonding was first reported in ref 15.

- (1) Waddington, T. C. *Trans. Faraday Soc.* **1959**, *55*, 1531.
- (2) Dasent, W. E. *Nonexistent Compounds; Compounds of Low Stability*; Marcel Dekker: New York, 1965.
- (3) *Gmelin Handbook, Au Suppl., Vol. B1*; Springer: Berlin, 1992; p 113.
- (4) Schröder, D.; Hrušák, J.; Tornieporth-Oelting, I. C.; Klapötke, T. M.; Schwarz, H. *Angew. Chem., Int. Ed. Engl.* **1994**, *33*, 212.
- (5) Evans, C. J.; Gerry, M. C. L. *J. Am. Chem. Soc.* **2000**, *122*, 1560–1561.
- (6) Seidel, S.; Seppelt, K. *Science* **2000**, *290*, 117.
- (7) Drews, T.; Seidel, S.; Seppelt, K. *Angew. Chem., Int. Ed.* **2002**, *41*, 454.
- (8) Hwang, I.-C.; Seidel, S.; Seppelt, K. *Angew. Chem., Int. Ed.* **2003**, *42*, 4392.
- (9) Seppelt, K. *Z. Anorg. Allg. Chem.* **2003**, *629*, 2427–2430.
- (10) Frenking, G. *Angew. Chem., Int. Ed.* **2003**, *42*, 143.
- (11) Gillespie, R.; Popelier, P. L. A. *Angew. Chem., Int. Ed.* **2003**, *42*, 3331.
- (12) Frenking, G. *Angew. Chem., Int. Ed.* **2003**, *42*, 3335.
- (13) Evans, C. J.; Gerry, M. C. L. *J. Chem. Phys.* **2000**, *112*, 1321–1329.

- (14) Evans, C. J.; Gerry, M. C. L. *J. Chem. Phys.* **2000**, *112*, 9363–9374.
- (15) Evans, C. J.; Lesarri, A.; Gerry, M. C. L. *J. Am. Chem. Soc.* **2000**, *122*, 6100–6105.
- (16) Evans, C. J.; Rubinoff, D. J.; Gerry, M. C. L. *Phys. Chem. Chem. Phys.* **2000**, *2*, 3943–3948.
- (17) Reynard, L. M.; Evans, C. J.; Gerry, M. C. L. *J. Mol. Spectrosc.* **2001**, *206*, 33–40.
- (18) Walker, N. R.; Reynard, L. M.; Gerry, M. C. L. *J. Mol. Struct.* **2002**, *612*, 109–116.
- (19) Thomas, J. M.; Walker, N. R.; Cooke, S. A.; Gerry, M. C. L. *J. Am. Chem. Soc.* **2004**, *126*, 1235–1246.
- (20) Cooke, S. A.; Gerry, M. C. L. *Phys. Chem. Chem. Phys.* **2004**, *6*, 3248.
- (21) Michaud, J. M.; Cooke, S. A.; Gerry, M. C. L. *Inorg. Chem.* **2004**, *43*, 3871.
- (22) Lovallo, C. C.; Klobukowski, M. *Chem. Phys. Lett.* **2002**, *368*, 589.

The “interaction strength”, as measured by the above parameters, increases in the orders $\text{Ar} < \text{Kr} < \text{Xe}$ and $\text{Ag} < \text{Cu} < \text{Au}$. Hitherto all possible NgM bonds in NgMX complexes have been reported except for XeCu and XeAu, which would clearly be the strongest and most interesting of them all. Now, recently, complexes containing such bonds have been observed. The spectra of XeCuX complexes will be reported elsewhere. The present paper is concerned with XeAuF.

XeAuF is also of interest in several other contexts. In 1995, Pyykkö predicted that the ions NgAu^+ and NgAuNg^+ should be stable, and that XeAu bond energies in XeAu^+ and XeAuXe^+ should be ~ 77 and ~ 106 kJ mol^{-1} , respectively.²³ Later, AuXe^+ was detected mass spectrometrically, and refined calculations carried out at the same time predicted a rather larger dissociation energy, ~ 127 kJ mol^{-1} , as well as $r_e = 2.57$ Å and $\omega_e \approx 149$ cm^{-1} .²⁴

In a recent review of the properties of all NgM^+ ions (M = any metal), Bellert and Breckenridge²⁵ noted that the bonding properties of such ions could be accounted for in terms of an electrostatic interaction, *except for those of* NgAu^+ (Ng = Ar, Kr, Xe) and especially XeAu^+ , where they entertained the possibility that Xe acts as a Lewis base. Since their conclusions were based on the above ab initio values, they appealed for further experimental data, particularly on AuXe^+ . Clearly, XeAuF is closely related and relevant.

Shortly after the report of ArAuCl and KrAuCl ,¹⁵ two further papers appeared. One reported detection of the molecule HArF in a matrix using infrared spectroscopy;²⁶ HArF was hailed as the first stable true Ar compound.²⁷ The other was ref 6, which reported the isolation of the compound $[\text{AuXe}_4^{2+}][\text{Sb}_2\text{F}_{11}^-]_2$ as solid crystals from which its geometry could be obtained by X-ray diffraction.⁶ It has been hailed as the first compound with a strong metal–xenon bond.²⁸ Interestingly, although both HArF and $[\text{AuXe}_4^{2+}][\text{Sb}_2\text{F}_{11}^-]_2$ evidently have chemical bonds to the noble gas, neither is truly stable: the former is stable only up to 27 K in an argon matrix, while the latter must be kept in a Xe atmosphere.

Several more compounds with XeAu bonds have now been isolated. Early results produced complexes with Au(II) and Au(III), with XeAu bond lengths ~ 2.66 – 2.71 and ~ 2.59 – 2.62 Å, respectively.⁷ More recently, the interesting Au(I) compound $[(\text{F}_3\text{As})\text{AuXe}^+][\text{Sb}_2\text{F}_{11}^-]$ has been isolated; in it $r(\text{XeAu}) = 2.607$ Å with an apparent $\nu(\text{XeAu}) \approx 138$ cm^{-1} .^{8,9} XeAuF is thus the second XeAu(I) complex to be reported. However, in contrast to the earlier complex, it is a neutral molecule. Because the samples are gaseous, the measured properties are those of isolated molecules without external influences. The high resolution of microwave spectroscopy has produced much more information than is available from one technique to more traditional synthetic chemists, including *experimental* bond lengths, vibration frequencies, and measures of electron distributions. The molecule is really a benchmark for all species containing XeAu bonds.

2. Experimental Methods

Details of the Balle–Flygare-type²⁹ Fourier transform microwave (FTMW) spectrometer in use at the University of British Columbia have been given earlier,³⁰ as have details of the laser ablation source.³¹ A pulse of radiation from a Nd:YAG laser (1064 nm) was focused onto a rotating, translating gold rod. The Au plasma reacted with a pulse of gas composed of 5% SF_6 and 15–20% Xe in Ar. The gas pulse was injected into the Fabry–Pérot cavity of the spectrometer by a Series 9 solenoid valve (General Valve Corp.); pressures within the backing gas reservoir were 5–7 atm. Free induction decays at rotational transition frequencies of XeAuF were collected following rotational polarization of the gas by microwave pulses. The time-domain signals were averaged and then converted to the frequency domain by fast Fourier transformation. The propagation of microwaves in the cavity occurred coaxial to the gas expansion. This configuration is optimal with respect to the sensitivity and resolution of the experiment and results in a doubling of each observed transition by the Doppler effect.

Spectra were observed between 6 and 26 GHz. In all cases line frequency measurements were referenced to a Loran frequency standard accurate to 1 part in 10^{10} . The observed line widths were ~ 7 – 10 kHz (fwhm), and the reported line frequencies have an estimated accuracy of ± 1 kHz.

3. Quantum Chemical Calculations

Although the results in ref 22 provided several useful parameters, notably bond lengths and dissociation energies, other useful results, such as valence orbital populations and MOLDEN plots, were not presented. Accordingly, a new set of MP2 calculations has been carried out using the GAUSSIAN 03³² suite of programs. For F the 6-311G** basis set was used. For Au and Xe pseudopotentials of the Stuttgart/Koeln group were used with corresponding basis sets. In the case of Xe the ECP46MWB scheme has been employed with the contraction (6s6p3d1f)/4s4p3d1f.^{33,34} For Au the ECP60MWB_MP2 (9s9p6d4f) scheme was used.³³ Basis set superposition error (BSSE) was accounted for using the counterpoise correction method of Boys and Bernardi.³⁵ The local energy density, $H_b(r)$ has been evaluated at the (3,–1) critical point located between the Xe and Au atoms using the AIMPAC software of Bader et al.³⁶

4. Results

4.1. Spectrum and Analysis. Estimates of rotational constants for various isotopomers of XeAuF were obtained using the ab initio bond lengths of ref 22. Initial experimental conditions for its preparation were predicted on the basis of the conditions required for the preparation of KrAuF^{19} and XeAgF^{20} . After several unsuccessful searches, two lines were eventually found at 10726.9 MHz. Lines in this region were

(23) Pyykkö, P. *J. Am. Chem. Soc.* **1995**, *117*, 2067.

(24) Schröder, D.; Schwarz, H.; Hrušák, J.; Pyykkö, P. *Inorg. Chem.* **1998**, *37*, 624.

(25) Bellert, D.; Breckenridge, W. H. *Chem. Rev.* **2002**, *102*, 1595–1622.

(26) Khriachtchev, L.; Pettersson, M.; Runenberg, N.; Lundell, J.; Räsänen, M. *Nature* **2000**, *406*, 874.

(27) Frenking, G. *Nature* **2000**, *406*, 836.

(28) Christe, K. O. *Angew. Chem., Int. Ed.* **2001**, *40*, 1419.

(29) Balle, T. J.; Flygare, W. H. *Rev. Sci. Instrum.* **1981**, *52*, 33.

(30) Xu, Y.; Jäger, W.; Gerry, M. C. L. *J. Mol. Spectrosc.* **1992**, *151*, 206–216.

(31) Walker, K. A.; Gerry, M. C. L. *J. Mol. Spectrosc.* **1997**, *182*, 178–183.

(32) Frisch, M. J.; Trucks, G. W.; Schlegel, H. B.; Scuseria, G. E.; Robb, M. A.; Cheeseman, J. R.; Montgomery, J. A., Jr.; Vreven, T.; Kudin, K. N.; Burant, J. C.; Millam, J. M.; Iyengar, S. S.; Tomasi, J.; Barone, V.; Mennucci, B.; Cossi, M.; Scalmani, G.; Rega, N.; Petersson, G. A.; Nakatsuji, H.; Hada, M.; Ehara, M.; Toyota, K.; Fukuda, R.; Hasegawa, J.; Ishida, M.; Nakajima, T.; Honda, Y.; Kitao, O.; Nakai, H.; Klene, M.; Li, X.; Knox, J. E.; Hratchian, H. P.; Cross, J. B.; Adamo, C.; Jaramillo, J.; Gomperts, R.; Stratmann, R. E.; Yazyev, O.; Austin, A. J.; Cammi, R.; Pomelli, C.; Ochterski, J. W.; Ayala, P. Y.; Morokuma, K.; Voth, G. A.; Salvador, P.; Dannenberg, J. J.; Zakrzewski, V. G.; Dapprich, S.; Daniels, A. D.; Strain, M. C.; Farkas, O.; Malick, D. K.; Rabuck, A. D.; Raghavachari, K.; Foresman, J. B.; Ortiz, J. V.; Cui, Q.; Baboul, A. G.; Clifford, S.; Cioslowski, J.; Stefanov, B. B.; Liu, G.; Liashenko, A.; Piskorz, P.; Komaromi, I.; Martin, R. L.; Fox, D. J.; Keith, T.; Al-Laham, M. A.; Peng, C. Y.; Nanayakkara, A.; Challacombe, M.; Gill, P. M. W.; Johnson, B.; Chen, W.; Wong, M. W.; Gonzalez, C.; Pople, J. A. *Gaussian 03*, revision B.01; Gaussian, Inc.: Pittsburgh, PA, 2003.

(33) Pseudopotentials of the Stuttgart/Koeln group (<http://www.theochem.uni-stuttgart.de/pseudopotentials>), 2003.

(34) Nicklass, A.; Dolg, M.; Stoll, H.; Preuss, H. *J. Chem. Phys.* **1995**, *102*, 8942.

(35) Boys, S. F.; Bernardi, F. *Mol. Phys.* **1970**, *19*, 553.

(36) Bader, R. F. W. (www.chemistry.mcmaster.ca/aimpac), 1995.

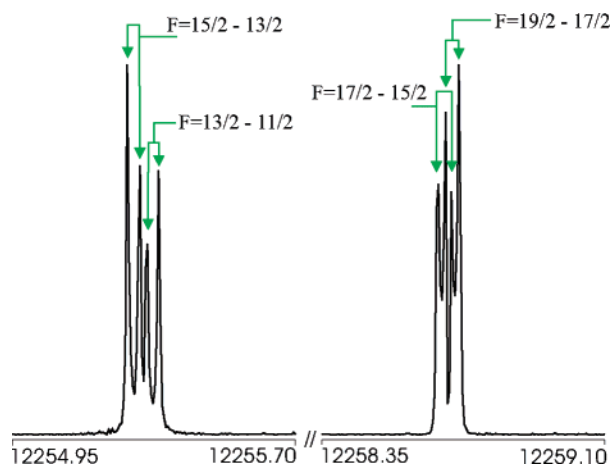


Figure 1. ^{197}Au hyperfine structure of the $J = 8-7$ transition of $^{129}\text{Xe}^{197}\text{Au}^{19}\text{F}$. The figure is a composite drawing, with each group recorded using 5000 averaging cycles taken over 4K data points. A 4K transform was used. Each line is doubled by the Doppler effect, as described in the text.

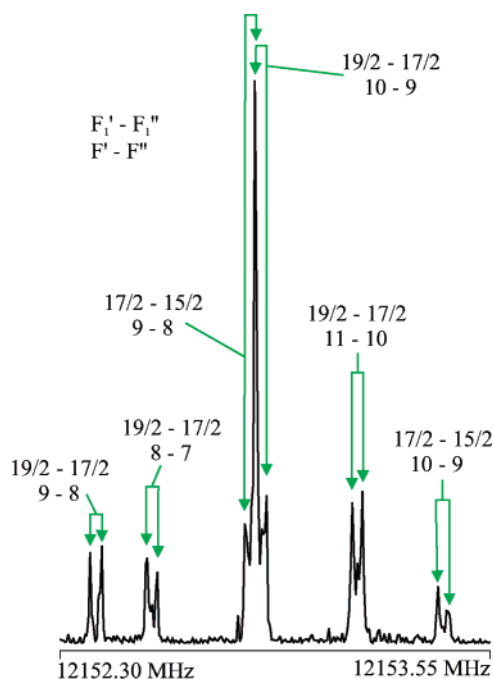


Figure 2. A portion of the hyperfine pattern of the $J = 8-7$ transition of $^{131}\text{Xe}^{197}\text{Au}^{19}\text{F}$. A total of 16 700 averaging cycles was recorded over 4K data points; a 4K transform was used. Each line is doubled by the Doppler effect, as described in the text.

anticipated to be $J = 7-6$ transitions, and accordingly a second group of lines was observed at 12 258.6 MHz, $2B_0$ higher in frequency than the first group. To be observed, both groups required laser ablation of the gold metal. Initially these groups of lines were thought to be carried by the $^{132}\text{XeAuF}$ isotopomer, and so further lines were sought on that basis. More transitions were found at 12 153.4 MHz. The frequency difference between this group and the previous group was consistent with an increase of two mass units on the Xe atom. The hyperfine structure of this group of lines was, however, too rich to be consistent with the carrier being $^{134}\text{XeAuF}$. Instead the lines were assigned to the $^{131}\text{XeAuF}$ isotopomer ($^{131}\text{Xe } I = 3/2$), suggesting that the first two groups of lines were from $^{129}\text{XeAuF}$. On this basis transitions from the $^{132}\text{XeAuF}$, $^{134}\text{XeAuF}$, and $^{136}\text{XeAuF}$ isotopomers were predicted and quickly found.

A total of 103 transitions was recorded from the five observed isotopomers. Examples are given in Figures 1 and 2. The former shows the ^{197}Au hyperfine structure of the $J = 8-7$ transition of $^{129}\text{XeAuF}$. The latter shows a portion of the hyperfine structure of ^{131}Xe and ^{197}Au in $J = 8-7$ of $^{131}\text{XeAuF}$. The measured frequencies together with the assignments are given in Table 1. For all but the $^{131}\text{XeAuF}$ isotopomer, the coupling scheme $J + I_{\text{Au}} = F$ was used. For $^{131}\text{XeAuF}$ the coupling scheme $J + I_{\text{Au}} = F_1$; $F_1 + I_{\text{Xe}} = F$ was used. The spectra were analyzed individually using Pickett's global least-squares fitting program, SPFIT.³⁷ Spectroscopic constants obtained from this fitting procedure are given in Table 2.

4.2. Structure. The basic pattern of the spectrum has established that XeAuF is linear; the bond lengths were determined from the rotational constants in Table 2. Because rotational transitions were observed only for molecules in the ground vibrational state, equilibrium (r_e) geometries were not available, and approximations were necessary. In addition, isotopic substitutions could not be made at either Au or F, and $r(\text{AuF})$ was set at its r_e value in AuF monomer.^{5,38} Because Xe was isotopically substituted, the XeAu bond length was evaluated from the spectra.

Geometries were obtained using three different approximations. The first produced the ground-state effective (r_0) structure. The bond lengths were obtained from a least-squares fit to the ground-state moments of inertia using the rigid rotor formula and assuming no vibrational dependence of I_0 :

$$I_0 = I_{\text{rigid}}(r_0) \quad (1)$$

In the second approximation the vibrational dependence was partially accounted for with an extra constant, ϵ , assumed to be the same for all isotopomers:

$$I_0 = I_{\text{rigid}}(r_{1\epsilon}) + \epsilon \quad (2)$$

Least-squares fits including ϵ as an extra parameter gave $r_{1\epsilon}$ bond lengths.³⁹ These are equivalent to earlier substitution (r_s) bond lengths⁴⁰ when a large enough data set is used. Finally, the mass dependence of ϵ was accounted for using⁴¹

$$I_0 = I_m + c(I_m)^{1/2} + d \left(\frac{m_1 m_2 m_3}{M} \right)^{1/2} \quad (3)$$

where c and d are fitting parameters. In an $r_m^{(1)}$ fit, d is set to zero; in an $r_m^{(2)}$ fit, both c and d are included. Here $I_m \equiv I_{\text{rigid}}(r_m)$; m_1 , m_2 , and m_3 are atomic masses; M is the molecular mass. This procedure, when applied to triatomics, has been shown by Watson et al.⁴¹ to give in many cases bond lengths which are excellent approximations to the equilibrium (r_e) values. Attempts at obtaining an $r_m^{(2)}$ geometry for XeAuF were unsuccessful because of the lack of isotopic data; uncertainties in c and d in the $r_m^{(2)}$ procedure were considerably larger than the parameter values themselves. The results of the other three fitting procedures are given in Table 3.

5. Discussion

5.1. Xenon–Gold Bond Length. In this section we consider the accuracy and validity of the experimental bond lengths, along

(37) Pickett, H. M. *J. Mol. Spectrosc.* **1991**, *148*, 371–377.

(38) Okabayashi, T.; Nakaoka, Y.; Yamazaki, E.; Tanimoto, M. *Chem. Phys. Lett.* **2002**, *366*, 406.

(39) Rudolph, H. D. *Struct. Chem.* **1991**, *2*, 581.

(40) Costain, C. C. *J. Chem. Phys.* **1958**, *29*, 864.

(41) Watson, J. K. G.; Roytburg, A.; Ulrich, W. *J. Mol. Spectrosc.* **1999**, *196*, 102.

Table 1. Measured Transition Frequencies for XeAuF

isotopomer	$J'-J''$	F'_1-F_1''	$F'-F''$	frequency (MHz)	obs – calc (kHz) ^a	isotopomer	$J'-J''$	F'_1-F_1''	$F'-F''$	frequency (MHz)	obs – calc (kHz) ^a		
¹²⁹ XeAuF	4–3		11/2–9/2	6132.9830	0.5	¹³² XeAuF	4–3		9/2–7/2	6054.0426	–2.6		
	5–4		9/2–7/2	7654.2800	–1.6		5–4			11/2–9/2	6054.1964	5.3	
				7/2–5/2	7654.5633			–1.1			9/2–7/2	7555.7839	1.6
				11/2–9/2	7663.7710			–0.7			7/2–5/2	7556.0704	1.4
	7–6			13/2–11/2	7663.8539		–0.7				11/2–9/2	7565.2802	0.8
				13/2–11/2	10722.3415		–0.1	8–7			13/2–11/2	7565.3650	1.5
				11/2–9/2	10722.4300		5.4				15/2–13/2	12097.6809	–0.0
				15/2–13/2	10726.8603		–0.3				13/2–11/2	12097.7336	–0.1
				17/2–15/2	10726.8957		0.2				17/2–15/2	12101.0889	2.8
			15/2–13/2	12255.2699	–0.3		9–8				19/2–17/2	12101.1073	–3.6
	8–7			13/2–11/2	12255.3209			–1.4			17/2–15/2	13610.6230	0.4
				17/2–15/2	12258.6750			2.0			15/2–13/2	13610.6570	–1.0
				19/2–17/2	12258.6945		–2.9			19/2–17/2	13613.2823	–0.4	
	9–8			17/2–15/2	13787.9108		1.9	10–9			21/2–19/2	13613.2991	–1.7
				15/2–13/2	13787.9419		–1.9				19/2–17/2	15123.3924	2.7
				19/2–17/2	13790.5665		–0.7		11–10			17/2–15/2	15123.4118
	10–9			21/2–19/2	13790.5845		–0.5				21/2–19/2	15125.5235	–3.5
				19/2–17/2	15320.3713		–1.5				23/2–21/2	15125.5400	–0.6
				17/2–15/2	15320.3983		1.0	12–11			21/2–19/2	16636.0363	–5.3
	11–10			21/2–19/2	15322.5058		–2.9				19/2–17/2	16636.0590	–0.7
				23/2–21/2	15322.5225		0.5				23/2–21/2	16637.7947	–2.8
				21/2–19/2	16852.7226		1.3			25/2–23/2	16637.8073	–0.6	
	12–11			19/2–17/2	16852.7445		5.4	13–12			23/2–21/2	18148.6103	–1.0
				23/2–21/2	16854.4739		–2.0				21/2–19/2	18148.6323	7.4
				25/2–23/2	16854.4861		–0.1				25/2–23/2	18150.0848	4.8
				21/2–19/2	18385.0062		5.7				23/2–21/2	19661.1137	–4.1
				25/2–23/2	18386.4531		–1.7		14–13			23/2–21/2	19661.1283
	13–12			27/2–25/2	18386.4638		0.9				27/2–25/2	19662.3634	–1.4
				25/2–23/2	19917.1824		–6.8				29/2–27/2	19662.3719	0.5
				23/2–21/2	19917.1928		–6.7	15–14			29/2–27/2	21174.6454	0.8
	14–13			27/2–25/2	19918.4354		0.0				31/2–29/2	21174.6552	5.3
				29/2–27/2	19918.4488		6.9				31/2–29/2	22686.9152	1.3
				27/2–25/2	21449.3394		0.4	16–15			33/2–31/2	22686.9228	4.5
			29/2–27/2	21450.4107	0.2					35/2–33/2	24199.1655	–6.5	
			31/2–29/2	21450.4165	0.7		¹³⁴ XeAuF		8–7		15/2–13/2	11996.2266	–0.9
	¹³¹ XeAuF	5–4		13/2–11/2	7598.4168			–1.3			13/2–11/2	11996.2809	0.1
					9/2–7/2			7589.7721	1.8			17/2–15/2	11999.6370
					10–9		10634.6782	–0.2	9–8			19/2–17/2	11999.6573
		7–6		17/2–15/2	12149.3040		–0.8				17/2–15/2	13496.4899	2.4
					13/2–11/2		12149.6244	0.4				15/2–13/2	13496.5217
					15/2–13/2		12149.9284	–3.3	¹³⁶ XeAuF	8–7		19/2–17/2	13499.1494
		8–7		13/2–11/2	12150.0235		–1.5					21/2–19/2	13499.1653
				9–8	12152.4054	0.6					15/2–13/2	11897.5622	1.9
				8–7	12152.5680	0.8			13/2–11/2	11897.6131	–1.0		
			17/2–15/2	12152.8557	2.9	9–8			17/2–15/2	11900.9700	2.2		
			19/2–17/2	12152.8864	0.7				19/2–17/2	11900.9899	–3.1		
			19/2–17/2	12153.1635	–1.1				17/2–15/2	13385.4866	–1.7		
9–8				17/2–15/2	12153.4149	0.6			15/2–13/2	13385.5247	0.4		
				21/2–19/2	13671.1567	0.6			19/2–17/2	13388.1506	0.4		
				21/2–19/2	13671.2748	0.6			21/2–19/2	13388.1695	0.9		
			11–10	13671.5556	–1.8								
			12–11	13671.7597	–1.5								
			11–10	13671.9465	2.6								

^a Observed – calculated residuals (kHz) using SPFIT program.

Table 2. Molecular Parameters for XeAuF

	B_0 (MHz)	D_J (kHz)	$eQq(\text{Au})$ (MHz)	$eQq(^{131}\text{Xe})$ (MHz)	rms ^a (kHz)
¹²⁹ XeAuF	766.096905(48) ^b	0.06916(17)	–527.637(79)		2.8
¹³¹ XeAuF	759.48101(21)	0.0674(15)	–527.45(13)	–134.54(18)	1.5
¹³² XeAuF	756.247472(44)	0.06753(14)	–527.704(79)		3.1
¹³⁴ XeAuF	749.90681(37)	0.0684(25)	–527.74(23)		1.7
¹³⁶ XeAuF	743.73989(37)	0.0664(25)	–527.67(23)		1.7

^a Root-mean-square deviations of the fit. ^b Numbers in parentheses are one standard deviation in units of the last significant figure.

with an interpretation of their values. Although the values of $r(\text{XeAu})$ obtained by the different methods vary by only 0.004 Å, they clearly depend on the assumption that $r(\text{AuF}) = 1.918$ Å. However, the results of the MP2 calculations in ref 22 agree exceedingly well. Since, however, the agreement is not so good for other complexes (ref 22, Tables 3–5), we note that the calculated change in AuF bond length on addition of Xe (ref 22, Tables 2 and 5) is –0.002 Å. We also note that if the AuF

bond length is held fixed at 1.916 Å (1.918–0.002 Å), then $r_m^{(1)}(\text{XeAu})$ alters by –0.0001 Å. Evidently the values of $r(\text{XeAu})$ in Table 3 are reliable.

In previous studies on the noble gas–noble metal halides,^{19,21} we have discussed the NgM bond length with respect to a covalent limit, $r_{\text{cov}}(\text{Ng}) + r_{\text{cov}}(\text{M}(\text{I}))$, and a van der Waals limit, $r_{\text{vdW}}(\text{Ng}) + r_{\text{ion}}(\text{M}^+)$. Trends observed have indicated that for

Table 3. Geometry^a of XeAuF

method	$r(\text{Xe}-\text{Au})$	$r(\text{Au}-\text{F})$	comments
r_0	2.548309(15) ^b	1.918 ^c	
r_{1e}	2.545675(9)	1.918 ^c	$\epsilon = 1.174(4) \text{ u}\text{\AA}^2$
$r_m^{(1)}$	2.543499(15)	1.918 ^c	$c = 0.0829(3) \text{ u}^{1/2}\text{\AA}$
MP2	2.545	1.922	ref 22
MP2	2.562	1.910	this work
$r_{\text{vdW}}(\text{Xe}) + r_{\text{ion}}(\text{Au}^+)$	2.95		
$r_{\text{cov}}(\text{Xe}) + r_{\text{cov}}(\text{Au(I)})$	2.57		
Standard Parameters (Å)			
	van der Waals	ionic	covalent
atom/ion	radius (r_{vdW})	radius (r_{ion})	radius (r_{cov})
Xe	2.18		1.30–1.31 ^d
Au ⁺ /Au(I)		0.77 ^e	1.27 ^f

^a Bond distances in Å. ^b Numbers in parentheses are one standard deviation in units of the last significant figure. ^c Au–F bond distance fixed at r_e of AuF.^{5,38} ^d Reference 42. ^e Value for coordination number 2 calculated from $r(\text{Au}^+) = r(\text{AuF}) - r(\text{F}^-)$. ^f Reference 43.

ArAgX, for example, $r(\text{ArAg})$ is closer to the van der Waals limit than the covalent limit, while for KrAuF, $r(\text{KrAu})$ is closer to the covalent limit.²¹ This is consistent with the trends of the “interaction strength” mentioned above, and it was expected that $r(\text{XeAu})$ would be closest of all to the covalent limit. Values in Table 3 show that $r(\text{XeAu})$ is much less than the van der Waals limit (by 0.4 Å), and in fact even shorter (by 0.03 Å) than the covalent limit!

Table 4 compares various properties, both experimental and ab initio, of XeAuF and a variety of related species. These include other NgMF molecules, XeAu⁺ and XeAuXe⁺ ions, and a range of other complexes reported to date containing XeAu bonds. The XeAu bond length in XeAuF fits squarely into the trends of the NgM bonds in NgMF. In addition, its value agrees well with the ab initio values. It is also close to the recent ab initio value of 2.57 Å for XeAu⁺,²⁴ and somewhat less than the 2.66 Å calculated for XeAuXe⁺.²³

At 2.54 Å, $r(\text{XeAu})$ in XeAuF is less than any other previously measured experimental value, regardless of the oxidation state of Au. The most valid comparison is with near-linear (F₃As)AuXe⁺, where $r(\text{XeAu}) = 2.61$ Å is longer by 0.07 Å; presumably the difference is related to the electronegativities of F and AsF₃. It is certainly not unreasonable to expect that if the XeAu bonds are dative bonds, then they should shorten when Au(I) is replaced by Au(II) and Au(III). This is not found, however, probably because in all known complexes with these oxidation states the coordination of Au is square planar. Simple geometrical calculations using the Xe–Xe hard-sphere distance or the Xe van der Waals radius show that $r(\text{XeAu}) < \sim 2.74$ Å is unlikely in AuXe₄²⁺, because of steric hindrance.²⁵ This is probably also a factor with the other complexes.

5.2. Flexibility and Bond Energy of XeAuF. The low value of the centrifugal distortion constant (~ 0.07 kHz) shows that XeAuF is remarkably rigid. The (XeAu) stretching frequency can be estimated using the diatomic approximation from

$$\omega_e = \left(\frac{4B^3}{D_J} \right)^{1/2} \quad (4)$$

The result is $\omega_e \approx 169 \text{ cm}^{-1}$, which is not unreasonable for a chemical bond involving heavy atoms; it agrees well with the ab initio value from the present work. This value is significantly

greater than that calculated for XeAu⁺ (149 cm^{-1} ²⁴), and for any experimental XeAu stretching frequencies measured to date. The comparisons are given in Table 4.

To obtain a mass-independent indication of the rigidity, the (XeAu) stretching force constant k_e has been evaluated, again in the diatomic approximation, using

$$k_e = \frac{16\pi^2\mu B^3}{D_J} \quad (5)$$

where

$$\mu = \frac{m^{\text{Xe}} m^{\text{AuF}}}{m^{\text{XeAuF}}} \quad (6)$$

is the reduced mass of XeAuF. The result is compared with corresponding values for other NgMF complexes in Table 4. By this measure XeAuF is by far the most rigid of these complexes. It should also be noted that k_e (137 N m^{-1}) is over 2 orders of magnitude larger than the corresponding value (0.6 N m^{-1}) for Ar–NaCl, an authentic, benchmark, van der Waals complex.⁴⁴

Table 4 also contains ab initio dissociation energies D_e for NgMF from ref 22. The value for XeAu in XeAuF has been confirmed by the calculations in the present work; the result is also given in Table 4. All are much greater than that of Ar–NaCl. The actual calculated value ($\sim 100 \text{ kJ mol}^{-1}$) is the greatest NgM bond energy obtained for all the NgMX complexes. It is, however, lower than all other reported values for XeAu bonds (Table 4); this may be the result of different calculation methods.

For all the NgMX complexes the NgM dissociation energies and stretching force constants are roughly proportional. XeAuF fits the general picture, as shown in Figure 3. This is consistent with the Morse potential, for which

$$D_e = \frac{k_e}{2\beta^2} \quad (7)$$

where β is the Morse potential constant. The force constants thus provide an approximate, but useful, *experimental* measure of the dissociation energies.

The XeAu bond energy is very large, and well into the realm of chemical bonds. (The mean KrF and XeF bond energies in KrF₂ and XeF₂ are 49 and 134 kJ mol^{-1} , respectively.⁴²) However, it would be well to consider whether it arises from a purely electrostatic interaction between Xe and AuF. For NgMX complexes reported earlier, rough estimates were obtained from the induction energies between Ng and MX, with the latter considered partially ionic according to the value of its dipole moment. Both dipole-induced dipole and charge-induced dipole values were obtained;^{19–21} corresponding calculations have been carried out for XeAuF.

(42) Bartlett, N.; Sladky, F. O. In *Comprehensive Inorganic Chemistry*; Bailar, J. C., Emelèus, H. J., Nyholm, R., Trotman-Dickenson, A. F., Eds.; Pergamon: Oxford, 1973.

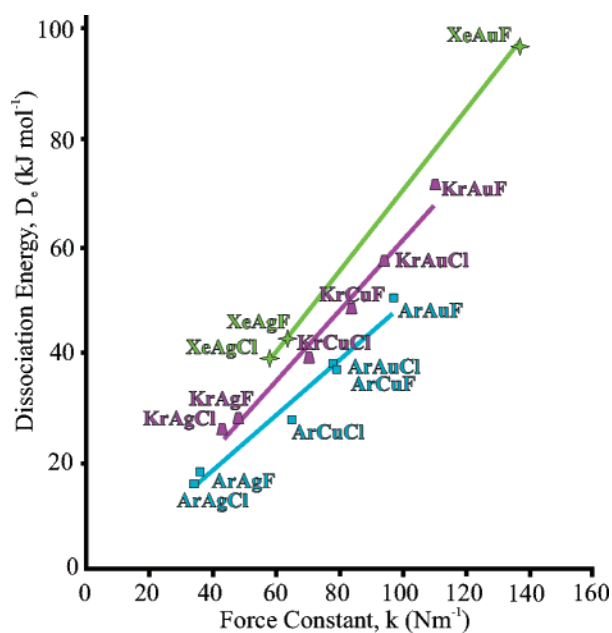
(43) Pyykkö, P. *Chem. Rev.* **1988**, *88*, 579.

(44) Mizoguchi, A.; Endo, Y.; Oshima, Y. *J. Chem. Phys.* **1998**, *109*, 10539.

Table 4. NgM Bond Lengths (r), Centrifugal Distortion Constants (D_J), NgM Stretching Frequencies (ω) and Force Constants (k), and Calculated NgM Bond Energies (D_e) of Xenon–Noble Metal Fluorides and Related Compounds and Complexes

compound or complex	$r(\text{NgM})$ (Å)		D_J (kHz) $\times 10^2$	$\omega(\text{NgM})$ (cm^{-1}) ^b	$k(\text{NgM})$ (N m^{-1}) ^b	D_e (kJ mol^{-1}) ^a
	expt	ab initio ^a				
ArCuF	2.22 ^c	2.24	94 ^c	224	79	37
KrCuF	2.32 ^d	2.32	38 ^d	185	84	48
ArAgF	2.56 ^e	2.59	95 ^e	141	36	18
KrAgF	2.59 ^f	2.61	31 ^f	125	48	28
XeAgF	2.65 ^g	2.68	14 ^g	130	64	43
ArAuF	2.39 ^h	2.40	51 ^h	221	97	50
KrAuF	2.46 ⁱ	2.45	16 ⁱ	176	110	71
XeAuF	2.54 ^j	2.55, 2.56 ^j	7 ^j	169 (165) ^k	137	97, 101 ^l
XeAu ⁺		2.57 ^l		149 ^l		127 ^l
XeAuXe ⁺		2.66 ^m		120, 182 ^{m,n}		108 ^m
Ar–NaCl	2.89 ^o			21 ^o	0.6 ^o	8 ^o
[F ₃ AsAuXe] ⁺	2.61 ^p	2.61 ^p		138 (148) ^p		137 ^p
[XeAuFAuXe] ³⁺	2.65 ^q			151, 101		
<i>cis</i> -[AuXe ₂] ²⁺	2.66 ^q					
<i>trans</i> -[AuXe ₂] ²⁺	2.71 ^q			121		
[AuXe ₄] ²⁺	2.74 ^r	2.79 ^r		129 ^r		~200
<i>trans</i> -[AuXe ₂ F] ²⁺	~2.6 ^q					
XeF ₂						134 ^s
KrF ₂						49 ^s

^a Values from ref 22 except where indicated. ^b Calculated from D_J using a diatomic approximation, except where indicated. ^c Reference 14. ^d Reference 21. ^e Reference 13. ^f Reference 18. ^g Reference 20. ^h Reference 16. ⁱ Reference 19. ^j This work. ^k Ab initio value in parentheses. ^l Reference 24. ^m Reference 23; D_e is one-half the atomization energy. ⁿ σ_g and σ_u values are given, respectively. ^o Reference 44; Ar–Na bond energy. ^p Reference 8; ab initio value in parentheses. ^q Reference 7. ^r Reference 6. ^s Reference 42; XeF and KrF bond energies.

**Figure 3.** Plots of the ab initio dissociation energies versus experimental stretching force constants for NgM bonds in NgMX complexes.

The calculations used the formulas⁴⁵

$$E_{\text{dip-ind.dip.}} = -\frac{\alpha_{\text{Xe}} D_{\text{AuF}}^2}{2\pi\epsilon_0 r_{\text{Xe,AuF}}^6} \quad (8)$$

and

$$E_{\text{chg-ind.dip.}} = -\frac{\alpha_{\text{Xe}} q_{\text{Au}}^2}{8\pi\epsilon_0 r_{\text{Xe,Au}}^4} \quad (9)$$

Here α_{Xe} is the polarizability of Xe; D_{AuF} is the dipole moment

(45) Berry, R. S.; Rice, S. A.; Ross, J. *The Structure of Matter: an Introduction to Quantum Mechanics*, 2nd ed.; Oxford: New York, 2002.

of AuF; q_{Au} is the charge on Au; $r_{\text{Xe,AuF}}$ is the distance between the Xe nucleus and the center of charge of AuF; and $r_{\text{Xe,Au}}$ is the XeAu internuclear distance. Equation 9 gives the leading term due only to the positive Au⁺ ion; its magnitude can be expected to be reduced by about 10% by the interaction with the negative F⁻ ion. Both calculations needed a value for D_{AuF} . Since it has not been measured, the value of 3.4 D estimated as described in ref 19 was used.⁴⁶ This in turn gave $q_{\text{Au}} = 0.37$ (ref 19, eq 8). With $\alpha_{\text{Xe}} = 4.04 \text{ \AA}^3$, the resulting values are $-E_{\text{dip-ind.dip.}} = 4 \text{ kJ mol}^{-1}$ and $-E_{\text{chg-ind.dip.}} = 11 \text{ kJ mol}^{-1}$. Both are very much less than the ab initio dissociation energies of $\sim 100 \text{ kJ mol}^{-1}$.

The induction energies of the NgMF complexes reported to date are compared in Table 5. The trends are clear, and XeAuF fits with them. The dipole–induced dipole terms are $\sim 35\%$ of the charge–induced dipole terms. Since the former are valid really only at long distances, so that effects of both ends of the dipole are comparable, the values of the charge–induced dipole terms are probably more reliable, and deductions will be based on them. Whereas for the CuF and AgF complexes $-E_{\text{chg-ind.dip.}}$ is $\sim 60\%$ of the dissociation energy, the value for the AuF complex is $\sim 10\%$. For the true van der Waals complexes Ar–NaCl and Ar–BeO, these values are 112% and 190%, respectively. Thus, in NgCuF and NgAgF it is improbable that the NgM bond is electrostatic. For NgAuF (and especially XeAuF) it is almost certainly *not* electrostatic.

For the record, the long distance approximation is suspect even for the charge–induced dipole term, which may thus be low by $\sim 50\%$. In addition, this term is only the leading term, and may provide only $\sim 50\%$ of the attractive energy.²⁵ However, there is also a large repulsive term which significantly

(46) Although D_{AuF} is small, it is not unreasonable. The procedure to obtain it was first to extrapolate the ionic characters i_c of AuCl and AuBr from their halogen eQq values⁵¹ to $i_c(\text{AuF}) \approx 0.5$. D_{AuF} was then estimated using eq 7 of ref 19 with the ionic polarizabilities given there. A corresponding calculation for AgCl gave $D_{\text{AgCl}} \approx 5.35 \text{ D}$, in error by $\sim 12\%$. If this is also the uncertainty in D_{AuF} and $q(\text{Au}^+)$, the induction energies (proportional to q^2) could be in error by $\sim 25\%$. The arguments given remain valid.

Table 5. Comparison of MX Dipole Moments and Effective Atomic Charges, Induction Energies, and ab Initio Dissociation Energies of NgMF and Related Complexes

complex	MX		$-E_{\text{ind}}^b$		D_e^b
	D^a	$q_{\text{Ng},\text{M}}^a$	dip.-ind.dip.	chg.-ind.dip.	
ArCuF	5.77 ^c	0.69	8	22	37
ArAgF	6.22 ^c	0.65	4	11	18
ArAuF	3.7 ^d	0.37	2	5	50
KrCuF	5.77	0.69	9	28	48
KrAgF	6.22	0.65	5	16	28
KrAuF	3.7	0.37	3	6	71
XeAgF	6.22	0.65	8	24	43
XeAuF	3.7	0.37	4	11	97 (101 ^e)
Ar-NaCl	9.00 ^f	0.79	4	10	8 ^g
Ar-BeO	7.20 ^h	0.84	26	84	45 ^h

^a D is the dipole moment of the MX monomer in Debye; q_{eff} in fractions of an elementary charge, estimated as described in text. ^b $-E_{\text{ind}}$ and D_e in kJ mol⁻¹; except where otherwise indicated, D_e is the NgM bond dissociation energy from ref 22. ^c Reference 47. ^d Estimated as described in the text and ref 19. ^e Value estimated in the present work. ^f References 48 and 49. ^g Reference 44. ^h Reference 50.

Table 6. ¹⁹⁷Au Nuclear Quadrupole Coupling Constants eQq (in MHz) for XeAuF and Related Species

molecule	$eQq(^{197}\text{Au})$	
	X = F	X = Cl
AuX	-53.2 ^a	9.6 ^b
ArAuX	-323.4 ^c	-259.8 ^d
KrAuX	-404.8 ^e	-349.9 ^d
XeAuX	-527.6 ^f	-
[XAuX] ⁻	-	-765 ^g
OCAuX	-1006 ^h	-1026 ^h

^a Reference 5. ^b Reference 51. ^c Reference 16. ^d Reference 15. ^e Reference 19. ^f This work. ^g Reference 52. ^h Reference 53.

reduces the total electrostatic energy (ref 25, Table 8). If all these caveats are included in a worst-case scenario, the electrostatic energy is still no greater than ~15% of the value of D_e in XeAuF.

5.3. Nuclear Quadrupole Coupling. Nuclear quadrupole coupling constants have been evaluated for both ¹⁹⁷Au and ¹³¹Xe in XeAuF. They are sensitive probes of the electron distributions at these nuclei, and in particular of how they change on complex formation.

Table 6 compares the ¹⁹⁷Au nuclear quadrupole coupling constants of monomeric AuX (X = F, Cl), corresponding NgAuX complexes, the isoelectronic XAuX⁻ ions, and the related OCAuX complexes. The changes on complexation with noble gas are large, consistent with a large change in the electron distribution, with the changes increasing in the order Ar < Kr < Xe. The actual amounts of change are the same for a given noble gas, regardless of the nature of X. For example, addition of Kr to AuF and AuCl changes $eQq(^{197}\text{Au})$ by -352 and -360 MHz, respectively. Since the latter is ~46% of the change when Cl⁻ is added to form ClAuCl⁻, we will assume the same applies to the fluoride. This would suggest the change when Xe adds to AuF is ~60% of the change expected when F⁻ adds to AuF to form FAuF⁻ (which is unknown). It is ~50% of the change when CO adds to AuF to form the strongly bonded complex OCAuF. The ¹⁹⁷Au coupling constants are consistent with the presence of an NgAu chemical bond in NgAuX, and in particular an XeAu chemical bond in XeAuF.

The same can be said for the ¹³¹Xe coupling constants. Table 7 presents values for a variety of molecules, in comparison with

Table 7. ¹³¹Xe Nuclear Quadrupole Coupling Constants (MHz) for Various Xe-Containing Species

molecule	$eQq(^{131}\text{Xe})$	ref
Xe	0	
Xe-Ne	0.39	54
Xe-Ar	0.72	54
Xe-Kr	0.70	54
Xe-HCl	-4.9	55
Xe-HF	-8.6	56
XeAgF	-82.8	20
XeAuF	-134.5	this work
XeH ⁺	-369.5	57
Xe[Kr]5s ² 4d ¹⁰ 5p ⁵ 6s ¹	-505	58

those of the Xe atom in its ground state and in an excited state with a half-empty p orbital. The coupling constant of ground-state atomic Xe is clearly zero because of its spherical symmetry. The slight distortions of its electron distribution in weakly bonded van der Waals complexes Xe-Ng and Xe-HX produce small ¹³¹Xe coupling constants. The complexes XeAgF and especially XeAuF have very large coupling constants; for the latter the value is ~25% of that of Xe with an electron removed from a 5p orbital.

As with the dissociation energies, it is necessary to check whether the large $eQq(^{131}\text{Xe})$ values are caused simply by polarization of the Xe atom by AuF. In the procedure used, which is outlined in ref 19, the field E_z and the field gradient E_{zz} due to AuF alone were first calculated. Following Sternheimer antishielding theory,⁵⁹⁻⁶¹ their values were then adjusted by including the polarized electrons. The equations used are

$$V_{zz} = (1 + \gamma^{\text{Xe}})E_{zz} + \epsilon^{\text{Xe}}E_z^2 \quad (10)$$

$$eQq(^{131}\text{Xe}) = -eQV_{zz} \quad (11)$$

Here γ^{Xe} and ϵ^{Xe} are Sternheimer antishielding parameters. For ¹³¹Xe, following ref 20, we used $138 \leq \gamma^{\text{Xe}} \leq 177$, and $\epsilon^{\text{Xe}} = -11.1 \text{ V}^{-1}$. (Note that for a p⁶ atom we have adopted the convention that $\gamma > 0$ and $\epsilon < 0$.⁶¹) Since, as was found earlier, the second term $\epsilon^{\text{Xe}}E_z^2$ in eq 10 is negligible,¹⁹⁻²¹ the deductions below result from the first term.

For NgMX, field gradients due to MX alone have been calculated using

- (47) Hoefl, J.; Lovas, F. J.; Tiemann, E.; Törring, T. *Z. Naturforsch.* **1970**, *25a*, 35.
- (48) Herbert, A. J.; Lovas, F. J.; Hollowell, C. J. M. C. D.; Story, T. L.; Street, K. *J. Chem. Phys.* **1968**, *48*, 2824.
- (49) DeLeeuw, F. H.; van Wachen, R.; Dymanus, A. *J. Chem. Phys.* **1969**, *50*, 1393.
- (50) Veldkamp, A.; Frenking, G. *Chem. Phys. Lett.* **1994**, *226*, 11.
- (51) Evans, C. J.; Gerry, M. C. L. *J. Mol. Spectrosc.* **2000**, *203*, 105.
- (52) Bowmaker, G. A.; Boyd, P. D. W.; Sorrenson, R. J. *J. Chem. Soc., Faraday Trans. 2* **1985**, *81*, 1627.
- (53) Evans, C. J.; Reynard, L. M.; Gerry, M. C. L. *Inorg. Chem.* **2001**, *40*, 6123.
- (54) Jäger, W.; Xu, Y.; Gerry, M. C. L. *J. Chem. Phys.* **1993**, *99*, 919-927.
- (55) Keenan, M. R.; Buxton, L. W.; Campbell, E. J.; Balle, T. J.; Flygare, W. H. *J. Chem. Phys.* **1980**, *73*, 3523-3529.
- (56) Baiocchi, F. A.; Dixon, T. A.; Joyner, C. H.; Klemperer, W. *J. Chem. Phys.* **1981**, *75*, 2041-2046.
- (57) Peterson, K. A.; Petrmichl, R. H.; McClain, R. L.; Woods, R. C. *J. Chem. Phys.* **1991**, *95*, 2352.
- (58) Faust, W. L.; McDermott, M. N. *Phys. Rev.* **1961**, *123*, 198.
- (59) Foley, H. M.; Sternheimer, R. M.; Tycko, D. *Phys. Rev.* **1954**, *93*, 734 and references therein.
- (60) Fowler, P. W.; Lasseretti, P.; Steiner, E.; Zanasi, R. *Chem. Phys.* **1989**, *133*, 121.
- (61) Fowler, P. W. *Chem. Phys.* **1989**, *156*, 494.

$$E_{zz} = -\frac{eq_M}{2\pi\epsilon_0 r_{NgM}^3} - \frac{eq_X}{2\pi\epsilon_0 r_{NgX}^3} \quad (12)$$

where q_M and q_X are the effective charges on the M and X ions and r_{NgM} and r_{NgX} are the NgM and NgX internuclear distances, respectively. The contributions of each term and their sums are given for all NgMX complexes observed to date in Table 8.

The eQq values obtained using eqs 10–12 are compared with the experimental values, also in Table 8. The calculated values are ~ 40 – 50% for NgCuX and NgAgX and $\sim 16\%$ for NgAuF. In no case, and especially not for NgAuF, does the calculated electrostatic value reach the experimental value. The relation parallels closely the one between the NgM induction energies and dissociation energies described earlier.

The simple theory of Townes and Dailey⁶² gives an estimate of the degree of donation of electron density from Xe to Au in XeAuF. The equation is

$$eQq = eQq_0 \left(n_\sigma - \frac{n_\pi}{2} \right) \quad (13)$$

where n_σ and n_π are the populations of the Xe $5p_\sigma$ and $5p_\pi$ orbitals in the complex, and eQq_0 is the coupling constant of a singly occupied $5p_\sigma$ orbital ($=505$ MHz from Table 6). If the donation is all σ donation, $n_\pi = 4$. With $eQq = -134.5$ MHz, this gives $n_\sigma = 1.73$, or a donation of 0.27 electron from Xe to Au.

5.4. Results of ab Initio Calculations. The numerical results of the ab initio calculations in the present work are distributed in Tables 3–5 and 9. Where they overlap with those of ref 22 they agree well. Essentially the same values are produced for the bond lengths (Table 3) and for the XeAu dissociation energy (Table 4); the bond lengths agree well with experiment. Essentially the same XeAu stretching frequency is determined from the experimental distortion constant as from the present ab initio calculation (Table 4).

In addition, both Mulliken and natural bond valence orbital populations have been calculated, with the main purpose of showing how they change on complex formation. The results are given in Table 9. Although the values differ in detail they indicate the same basic trend: a significant donation of σ -electron density from Xe to Au. The charges on Xe in the complex summarize the degree of donation (0.26 and 0.16 of an elementary charge for the Mulliken and natural bond populations, respectively). Comparison of the natural bond populations with those of XeAgF in ref 20 shows an increase in donation of ~ 0.1 electron in XeAuF. A similar comparison with the Mulliken populations of KrAuF in ref 19 also shows a greater donation of ~ 0.1 electron in XeAuF. Both these comparisons fit the expected trend in which the degree of noble gas–noble metal interaction should be greatest for XeAu bonds.

There is also an illuminating comparison with the Mulliken charges of ~ 0.4 electron calculated for Xe in $AuXe_4^{2+}$.⁶ The corresponding value in XeAuF (0.26 electron) is very comparable, especially considering that the oxidation states of Au are (II) and (I) for the ion and complex, respectively. Unfortunately, a corresponding value was not published for $F_3AsAuXe^+$.⁸

MOLDEN plots of contours of electron density of the 6σ and 3π valence MOs are presented in Figure 4. Both orbitals

Table 8. ⁸³Kr and ¹³¹Xe Nuclear Quadrupole Coupling Constants Resulting from Polarization Due to External Charges, in Comparison with Experimental Values, for NgMX Complexes

complex	q_{eff}^a	$E_{zz}(M)$	$E_{zz}(X)$	E_{zz}^b	$eQq(\text{Ng})$ (MHz)	
					calcd ^c	exptl
KrCuF	0.69	−1.592	0.295	−1.297	63	128.8
KrAgF	0.66	−1.092	0.202	−0.890	43	105.10
KrAuF	0.37	−0.715	0.127	−0.588	29	185.94
XeAgF	0.65	−0.992	0.187	−0.805	−35	−82.8
XeAgCl	0.56	−0.812	0.130	−0.681	−30	−78.2
XeAuF	0.37	−0.646	0.120	−0.526	−23	−134.54

^a Fractional charge on the M⁺ and X[−] ions (Table 5). ^b E_{zz} is the sum of $E_{zz}(M)$ and $E_{zz}(X)$, the field gradients at the Ng nucleus due to M⁺ and X[−] individually. ^c Calculated using eqs 10 and 11, with $\gamma = 78$ for Kr and 158 for Xe. For the Xe coupling constants the uncertainty is $\pm \sim 4$ MHz. The second term of eq 10 is negligible.

Table 9. Mulliken and Natural Bond Valence Orbital Populations and Charges, Q, for Xe, AuF, and XeAuF^a

	Mulliken		natural bond orbital	
	Xe + AuF	XeAuF	Xe + AuF	XeAuF
Xe				
q^a	0	0.26	0	0.16
n_s	2.00	1.94	2.00	1.97
n_{p_s}	2.00	1.76	2.00	1.86
n_{p_p}	4.00	3.98	4.00	4.00
Au				
q	0.57	0.33	0.77	0.60
n_s	0.46	0.60	0.41	0.62
n_{p_s}	0.05	0.24	0.01	0.01
n_{p_p}	0.08	0.08	0.02	0.03
n_{d_s}	1.78	1.68	1.80	1.75
n_{d_p}	4.03	4.01	3.99	3.98
n_{d_d}	4.00	4.00	4.00	4.00
F				
q	−0.57	−0.59	−0.77	−0.76
n_s	2.00	2.02	1.98	1.96
n_{p_s}	1.70	1.71	1.80	1.82
n_{p_p}	3.87	3.86	3.98	3.98

^a The units of q are fractions of the elementary positive charge e .

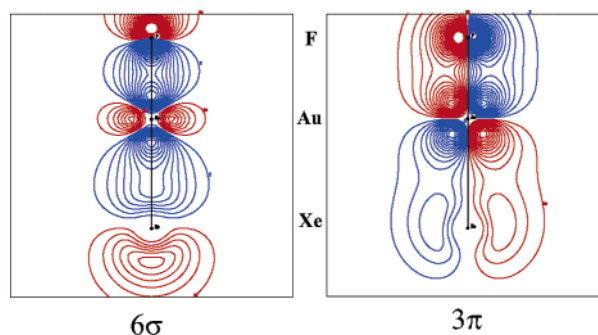


Figure 4. MOLDEn contour diagrams of two occupied valence molecular orbitals of XeAuF; in each case the value of the contours is $0.02n$, with $n = 1$ – 25 . The different colors indicate opposite signs of the wave functions.

are fully occupied. These plots suggest significant sharing of electron density between $5p$ orbitals on Xe and $5d$ orbitals on Au. (The 6σ orbital also has significant Au($6s$) character.) The σ -sharing is greater than the π -sharing; such sharing would seem to be a requirement for covalent bonding. The plots are comparable to those for the corresponding orbitals of KrAuF presented in ref 19, though the overlap appears to be a little less in XeAuF. It should be noted that we have *not* been able to construct MOs with comparable sharing for the accepted van der Waals complexes Ar–BeO and Ar–NaCl.

(62) Townes, C. H.; Dailey, B. P. *J. Chem. Phys.* **1949**, *17*, 782.

A criterion for covalent bonding suggested by Cremer and Kraka,⁶³ and reviewed by Frenking and Cremer,⁶⁴ is the energy density distribution ($H_b(r)$) at the bond critical point located along the path of maximum electron density (MED) between the two atoms. A negative value of $H_b(r)$ implies that potential energy dominates so that electron density builds up and a covalent bond is formed. For XeAuF the MED path is a straight line between the nuclei; at the XeAu bond critical point, $H_b(r) = -0.18$ hartree \AA^{-3} , consistent with a weak XeAu covalent bond.

The negative $H_b(r)$ is, however, unsurprising. Frenking and Cremer also point out (ref 64, pp 46–50) that where an ab initio dissociation energy is significantly greater than a charge-induced dipole induction energy, a negative $H_b(r)$ will be found, and covalent bonding can be assumed. As is shown in section 5.2, this is clearly the case for XeAuF.

6. Conclusion

The complex XeAuF has been detected and characterized in the gas phase using microwave rotational spectroscopy. In the hierarchy of noble gas–noble metal halide complexes it was expected to be the most strongly bonded; this has turned out to be the case.

The XeAu bond is short, at 2.54 \AA . It is also rigid, and has the largest stretching force constant of any NgM bond. The force constant correlates well with the ab initio bond energy, ~ 100 kJ mol^{-1} (Table 4, column 7), which is also the largest for any NgM bond in the NgMX series. The rearrangement of electron density on complex formation, at both the noble gas (Xe) and the metal (Au), is larger than that found for any other NgMX complex.

The properties of XeAuF are generally consistent with those of other molecules containing XeAu bonds.^{6–9} However, the XeAu bond length is the shortest reported, and the stretching frequency is among the highest. Interestingly, the ab initio dissociation energy is among the lowest reported for XeAu bonds.

From the outset the nature of the NgM bonds in NgMX complexes has been of primary interest. The bonding is clearly much stronger than that of conventional van der Waals bonds, in which individual molecules or atoms rest against each other,

and are held together by electrostatic forces. A starting point for discussion is to consider NgM to be at the border between van der Waals and chemical bonding. From the trends found for other complexes, XeAu was expected to give the most convincing evidence of chemical bonding.

Again XeAuF has largely fulfilled expectations. The XeAu bond length is at, or less than, the sum of Xe and Au(I) covalent radii. The ab initio dissociation energy (consistent with the XeAu stretching constant) is 10 times the charge-induced dipole induction energy. The change in the ¹⁹⁷Au nuclear quadrupole coupling constant on complex formation is at least 50% of that found when accepted chemical bonds (AuX⁵² or AuCO⁵³) are formed. A very large ¹³¹Xe coupling constant has been measured, which also cannot be accounted for in terms of simple electrostatic forces. It suggests a donation of ~ 0.27 electron from Xe to Au. The ab initio Mulliken and natural bond populations suggest a comparable donation. MOLDEEN plots of occupied valence MOs suggest significant electron sharing between Xe and Au. There is a negative energy distribution at the bond critical point. All these observations point to XeAu chemical bonds, indeed covalent bonds.⁶⁵

Although they vary in degree, the physical properties of all the NgMX complexes are essentially the same: they all have short, rigid NgM bonds, significant rearrangement of electron distribution on complex formation, and relatively large NgM dissociation energies. Neither of the last two properties can be fully accounted for solely with electrostatics. MOLDEEN plots of occupied valence MOs suggest electron sharing involving d orbitals on the metal. If it is the case that chemical, probably covalent, XeAu bonding is found in XeAuF (and the evidence strongly supports this conclusion), then there is NgM chemical bonding, to a greater or lesser degree, in *all* the NgMX complexes.

Acknowledgment. This research has been supported by the Natural Sciences and Engineering Research Council of Canada.

JA044955J

(65) It is possible to query whether the XeAu bond is covalent if $r(\text{AuF})$ is unchanged on complexation. However, this idea is unfounded, for such a change is not *necessary* for chemical bond formation. In the carbonyl analogues, OCMX, recently studied by us,^{53,66,67} several MX bond lengths do change (by up to 0.02 \AA in both directions). On the other hand, the CO bond lengths are unchanged (!) even though the OC–M bond is unquestionably covalent.

(66) Walker, N. R.; Gerry, M. C. L. *Inorg. Chem.* **2001**, *40*, 6158.

(67) Walker, N. R.; Gerry, M. C. L. *Inorg. Chem.* **2002**, *41*, 1236.

(63) Cremer, D.; Kraka, E. *Angew. Chem.* **1984**, *96*, 612; *Angew. Chem., Int. Ed. Engl.* **1984**, *23*, 627.

(64) Frenking, G.; Cremer, D. *Struct. Bonding* **1990**, *73*, 18–95.